Acta Biomed 2019; Vol. 90, Supplement 5: 9-19 DOI: 10.23750/abm.v90i5-S.8343

Review

Relationship between diagnostic imaging features and prognostic outcomes in gastrointestinal stromal tumors (GIST)

Ginevra Danti[1], Gloria Addeo[1], Diletta Cozzi[1], Nicola Maggialetti[2], Monica Marina Lanzetta[1], Gianluca Frezzetti[1], Antonella Masserelli[1], Silvia Pradella[1], Andrea Giovagnoni[3], Vittorio Miele[1]

[1] Department of Radiology, Careggi University Hospital, Florence, Italy; [2] Department of Medicine and Health Sciences "V. Tiberio", University of Molise, Campobasso, Italy; [3] Department of Radiology, Università Politecnica delle Marche, Ancona, Italy

Summary. Gastrointestinal stromal tumors (GISTs), the most frequent mesenchymal neoplasms of the gastrointestinal tract, are a relatively recently described entity. GISTs can occur across any age but are more common in patients older than 50 years. GISTs most commonly are in the stomach (60-70%), followed by the small intestine (20%-30%); they also rarely occur in the abdominal cavity, such as in the mesentery, the omentum and the retroperitoneum. Contrast-enhanced multi-detector computed tomography (MDCT) is the most largely used imaging modality for the localization, characterization and staging of GISTs. All patterns of enhancement on contrast-enhanced MDCT can be seen with GISTs, including hypoenhancing, isoenhancing, and hyperenhancing neoplasms. A lot of prognostication systems have been proposed for the risk stratification of GISTs. This review outlines the relationship between different diagnostic imaging features and prognostic outcomes in GISTs. (www.actabiomedica.it)

Key words: gastrointestinal stromal tumors, imaging features, computed tomography, prognostication system, outcome

Introduction

Gastrointestinal stromal tumors (GISTs) are the most frequent mesenchymal tumors of the gastrointestinal tract, they are thought to arise from the interstitial cells of Cajal, which are intestinal pacemaker cells that allow peristalsis and segmentation of the smooth muscle (1-3).

Rubin et al. in their study said that GISTs have no predilection for either sex, and although they occur over a wide age distribution, in fact about 75% are diagnosed in patients older than 50 years (4). These tumors can arise everywhere in the gastrointestinal tract, but their most common locations are the stomach (60-70%) and the small bowel (20-30%) (5-7). About 5% of GISTs are in the colon and rectum, another 5% in the esophagus (4, 8-11). A small part of these tumors also develops within the mesentery, omentum, retroperitoneum, and pelvis (E-GIST) (12, 13).

Usually patients have non-specific symptoms including early satiety, bloating, gastrointestinal bleeding, fatigue from anemia, or obstruction (14). Bleeding can take the form of slow, intraluminal gastrointestinal bleeding or massive intraperitoneal bleeding following the rupture and can be seen regardless of the enhancement pattern (15). Aggressive GISTs have a defined pattern of metastasis to the liver or throughout the abdomen (usually as multiple serosal-based nodules), or

both (5). Contrasting GISTs in elderly patients, lymphatic metastases represent a common route of initial spread in young patients (< or = 40 years) (16). Extra-abdominal diffusion is mainly to the lungs and bone but isn't usual (17). Gold et al. showed that a lot of patients have localized disease (79.4%), but approximately 11.4% have regional-distant metastatic disease at the time of presentation; recurrences have been reported up to 30 years after initial diagnosis and resection (18).

GISTs have the classic tendency of exophytic growth, especially since they arise from the outer muscular layer. There is frequently some growth towards the lumen however, as up to 50% of GISTs will exhibit mucosal ulceration on the luminal surface. Among other macroscopic characteristics, there can be focal areas of hemorrhage, necrosis, calcifications, intralesional cavitation or cystic degeneration (19).

Histologically, GISTs can be classified into three main subtypes: spindle cell type (most common, 70%), epithelioid type (20%), and mixed (10%). The cellularity is also highly variable, passing from hypocellular to highly cellular with high mitotic rates (20, 21).

Kindblom et al. in their study described that GISTs can have many histological patterns and can be positive for c-KIT (95%), CD34 (60-70%), ACAT2 (smooth muscle actin; 30-40%), S100 (5%), DES (desmin; 1-2%), and keratin (1-2%) (22-25).

Zao et al. showed how C-KIT is the most specific and sensitive marker in differentiating GISTs from other entities (20). Mol et al. described how C-KIT positive tumors benefit from system therapy with imatinib mesylate, defined as a target therapy (26-28). However, a subset of the 5% of tumors that are c-KIT-negative might benefit from c-KIT-targeted therapy (29).

The wide range of clinical presentations along with non-specific symptoms can pose a challenge in differential diagnosis of GISTs. To date contrast-enhanced multi-detector computed tomography (MDCT) is the most largely used imaging modality for the localization, characterization and staging of GISTs (30).

In fact radiologists have a leading role in timely and accurate diagnosis for the frequent tumor's variability in relation to location, pattern of enhancement, and other imaging features such as necrosis or cavitation.

Prediction of prognosis of primary tumors has been studied intensively. In their study Fletcher et al. proposed tumor size and mitotic activity as the two main factors for the risk stratification system (23).

We considered the correlation between AFIP criteria and MDCT features of GISTs; evaluating mitotic count and tumor size, this system incorporated tumor location as an additional variable and stratified prognosis of GISTs into 5 classes (none, very low, low, moderate, high) (31).

In this review of recent literature, we evaluated how some CT features such as location, size, margins, contrast enhancement are closely related to the malignancy risk and therefore to the outcome.

Imaging features

Cross-sectional imaging techniques are largely used for a variety of conditions and diseases both for diagnostic and interventional purposes (32-49). Ultrasonography is a radiation-free and well-tolerated imaging examination (50-53), but has a limited role in gastrointestinal pathology (54-61). MR has an excellent soft tissue contrast (62-65), but contrast-enhanced MDCT is the preferred technique for the diagnosis, staging and follow-up (66-73). The aspect of GISTs on imaging is highly variable with regards to location, relation to stomach-bowel wall, size, margins, pattern of enhancement and other imaging features that modify homogeneity of the lesion at non contrast-enhanced MDCT (hemorrhage, necrosis, calcifications, intralesional cavitation and cystic degeneration) (74, 75).

At the time of diagnosis with imaging GISTs could have variable dimensions range, measuring less than 1 cm to very large lesions measuring upwards of 35 cm (median 5 cm) (15). The tumors generally present as single nodules but they can consist also of multiple nodules. They are usually solid but can have central cystic degeneration. Calcification is an unusual feature of GISTs; it may occur in a smudged pattern or be present extensively throughout the tumor (Fig. 1) (22-24). Sharp et al. in their cases showed that central areas of low attenuation coincide with hemorrhage, necrosis, or cyst formation (76). Scatarige et al. said that lesions with extensive hemorrhage or necro-

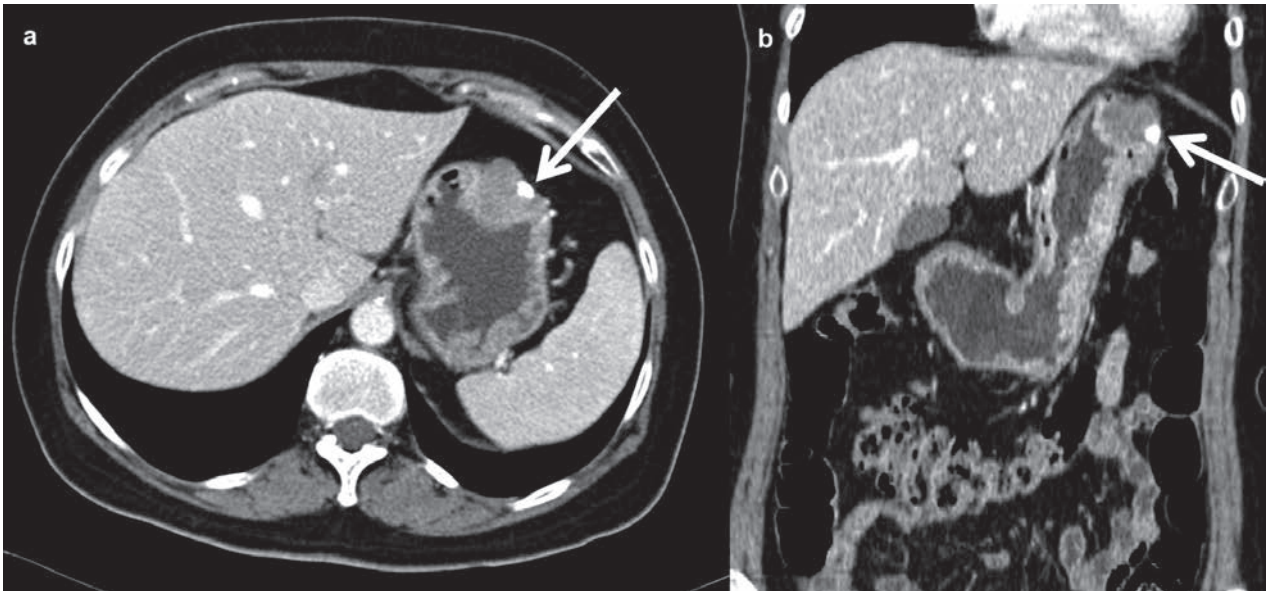

Figure 1. Axial (a) and coronal (b) contrast enhanced MDCT images in the portal venous phase show an intraluminal mass of gastric corpus (white arrows). This GIST presents heterogeneous contrast enhancement, irregular margins and size < 5 cm with centimetric intralesional calcification

sis may form large cystic spaces or cavities which may communicate with the gastro-intestinal lumen (77).

Through evaluation with contrast-enhancement MDCT, these tumors may show smooth and regular margins or irregular and jagged borders (78, 79) (Fig. 2, Fig. 3).

All patterns of enhancement on contrast-enhanced MDCT can be seen with GISTs, including hypoenhancing, isoenhancing, and hyperenhancing neoplasms (Fig. 4).

A peripheral enhancement pattern is present in the majority (92%) of cases on contrast-enhanced MDCT images. Homogeneous enhancement is present in a small part (8%) of cases (80). Contrast-enhanced MDCT may also demonstrate evidence of adjacent organ invasion, ascites, omental and peritoneal diffusion of tumor, or liver metastases (81-83) (Fig. 5, Fig. 6).

Prognostic system

Numerous prognostic systems have been proposed for the assessment of disease progression risk of GISTs, defined as the appearance of metastasis or tumor-related death. The most widely used systems today are the AFIP, the NIH, Joensuu modified NIH, and the Memorial Sloan Kettering Cancer Center nomogram.

The AFIP criteria were developed by Miettinen et al. in 2006 and based on previous AFIP studies reporting on 1055 gastric, 156 duodenal, 906 jejunal/ileal and 144 colorectal GISTs with no statistical validation.

Nevertheless, it remains uncertain which system is the most accurate. More validation and comparison studies are required to determine the optimal prognostic system for GISTs (23, 30, 84).

Imaging vs Prognosis

In the assessment of risk stratification, the AFIP criteria allow to subdivide these neoplasms in relation to the site of origin, GISTs located in the stomach turn out to be the least aggressive, followed by the duodenum or rectum and jejunum or ileum, characterized by greater risk of progression (85, 86).

One of the three main prognostic factors in Miettinen classification is tumor size: tumors smaller than 5 cm have a favorable prognosis, intermediate

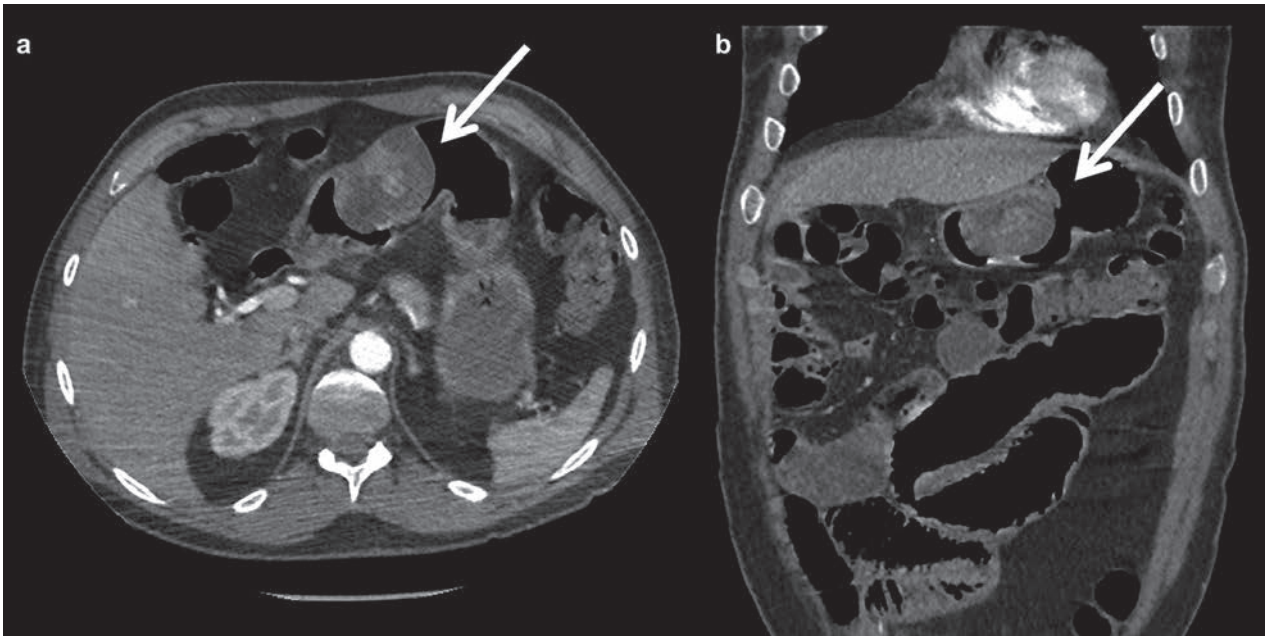

Figure 2. Axial (a) and coronal (b) contrast enhanced MDCT images in the arterial phase demonstrate a voluminous GIST on the anterior wall of gastric corpus (white arrows). The lesion shows heterogeneous contrast enhancement, regular margins and size > 5 ≤ 10 cm

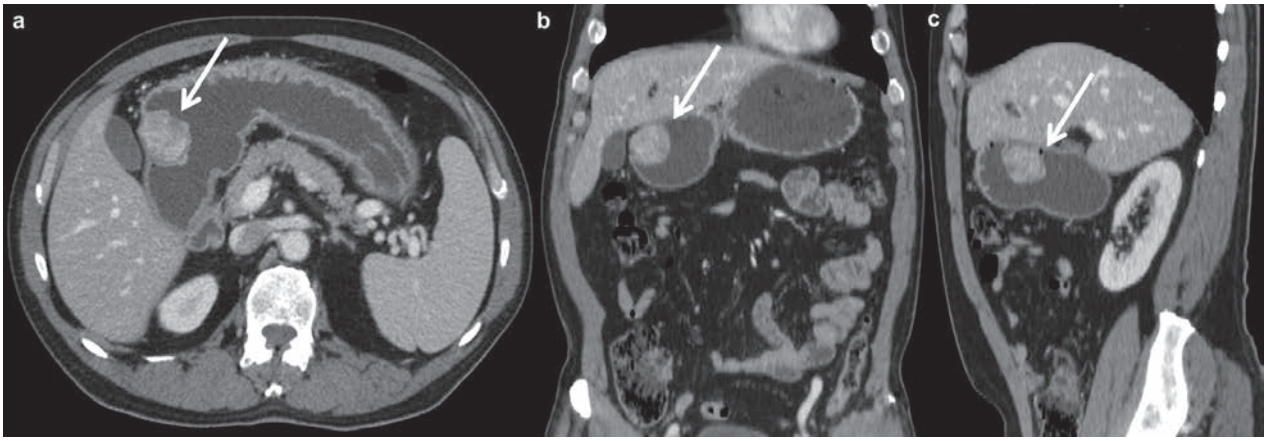

Figure 3. Axial (a), coronal (b) and sagittal (c) contrast enhanced MDCT images in the portal venous phase demonstrate an intraluminal mass of gastric corpus (white arrows). The lesion presents heterogeneous contrast enhancement, irregular margins and size < 5 cm.

between 5 and 10 cm and unfavorable greater than 10 cm (31).

Another important aspect to stress is the significant associations of several MDCT features with the size of the tumor. Some MDCT features could be observed more frequently with increasing tumor size. In fact neoplasm size seems to be statistically significantly associated with the pattern of contrast enhancement, necrosis, the shape of margins and adjacent organ invasion (76).

Zhou et al. in their study demonstrated that the analysis of the distribution of all these parameters among the different classes of size showed that heterogeneous contrast enhancement, irregular margins, and the other previously mentioned features (hemorrhage, necrosis, intralesional cavitation, cystic degeneration)

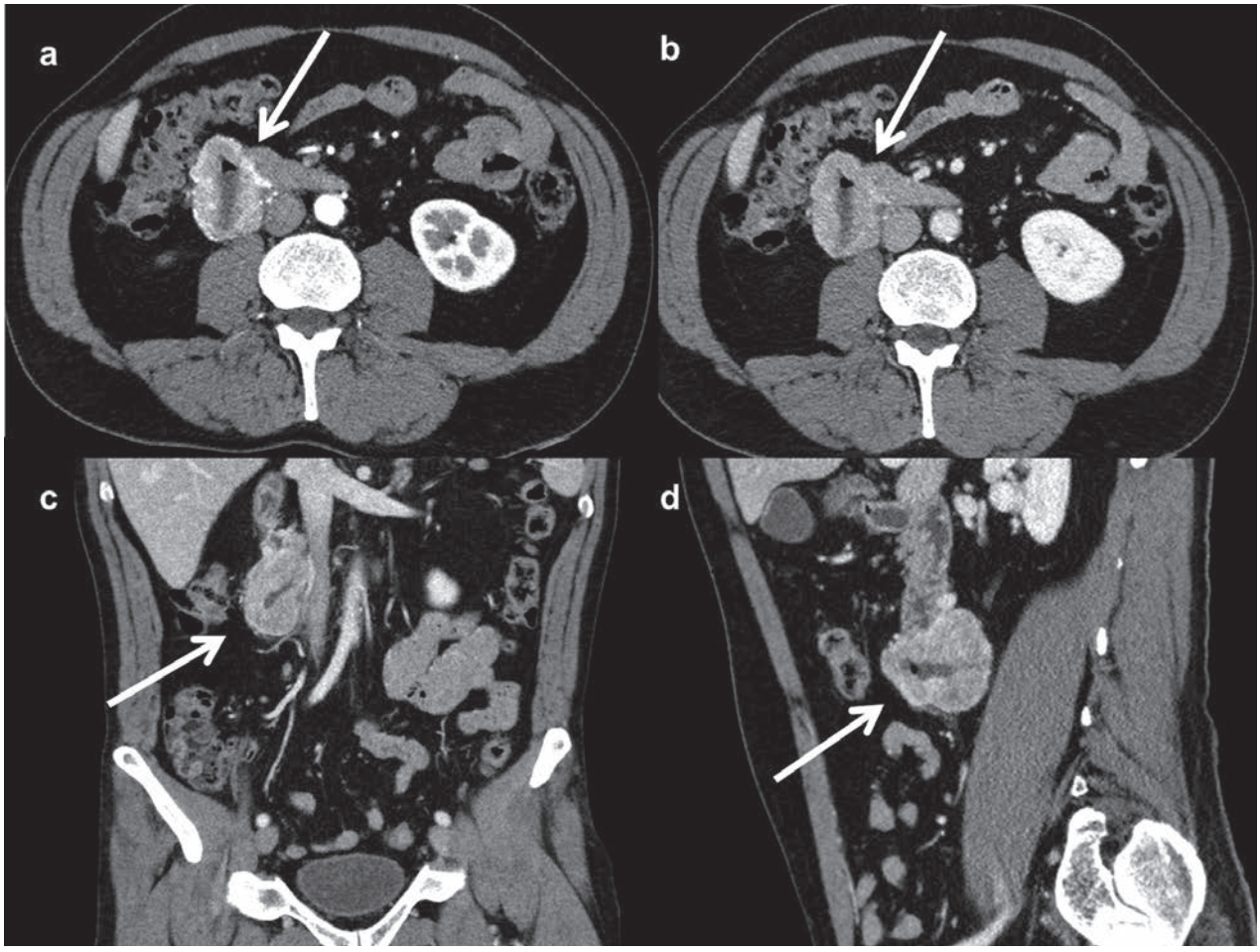

Figure 4. Axial (a,b), coronal (c) and sagittal (d) contrast enhanced MDCT images in the arterial (a) and the portal venous phase (b,c,d) show an exophytic mass of the duodenum (white arrows), strictly adjacent to the inferior vena cava. This GIST presents heterogeneous contrast enhancement, irregular margins, size > 5 ≤ 10 cm and a central area with necrosis and cavitation

trend to grow up with the increase of the size of tumor, being mostly detected in tumors sized 5 to 10 and greater than 10 cm (87-90).

The presence of single or multiple nodules is not correlated with an increased risk of disease progression. The finding of intralesional calcifications seems to be an aspecific parameter and not related to the prognosis. On the other hand, hemorrhage, necrosis, intralesional cavitation and cystic degeneration are associated with an increased risk of malignancy and therefore of disease progression (91).

Moreover, a significant association has been observed between shape of lesion margins and mitotic index (closely related to the outcome): most of lesions with a number of mitoses less than or equal to 5/50 HPFs showed regular margins, suggesting that solid lesions with smooth and not crispy borders could be less aggressive than the ones with jagged borders (75, 80). The presence of irregular margins showed a linear correlation with the risk classes, as it was absent in the none, very low, and low classes, whereas it could be observed in the moderate class and in high class (75, 80). In fact the mean number of mitoses was higher among the lesions with irregular margins compared with the mean value of mitoses detected in neoplasms showing regular margins (80, 92-95).

Many studies demonstrate that the presence of heterogeneous pattern of contrast enhancement is mainly observed in GISTs belonging to the moderate and high classes of risk. On the other hand, tumors

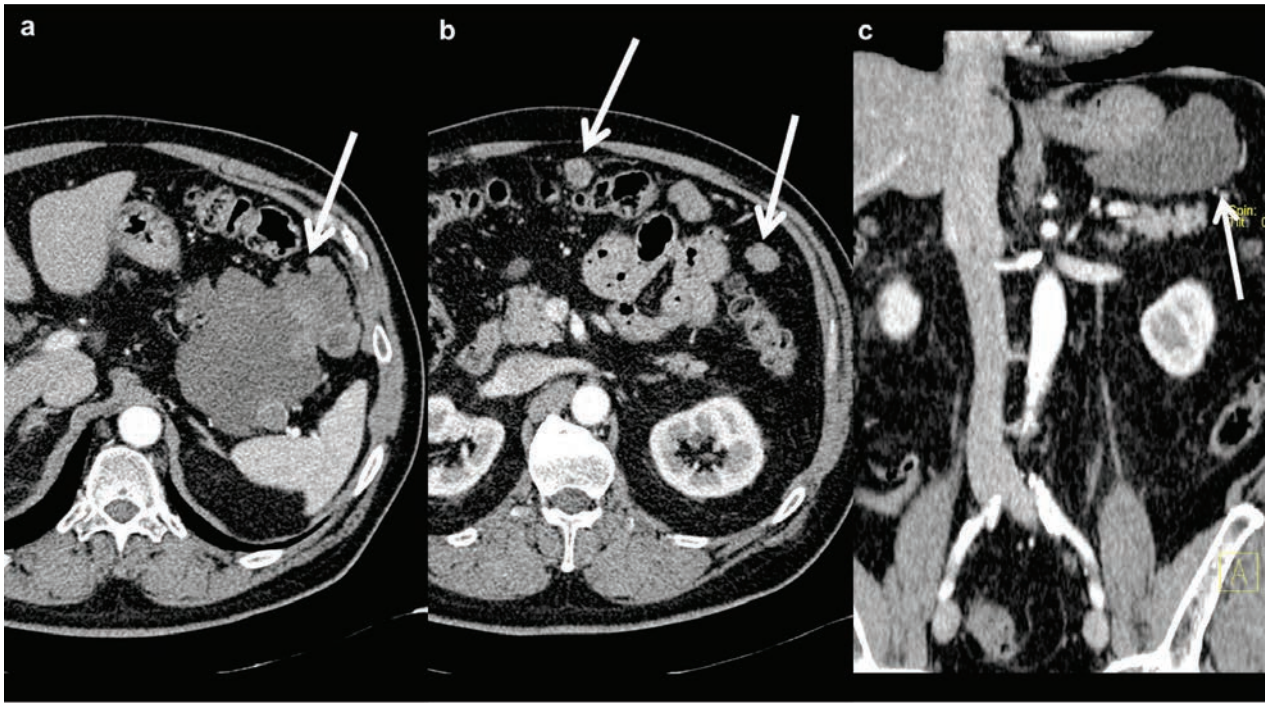

Figure 5. Axial (a) and coronal (c) contrast enhanced MDCT images in the arterial phase demonstrate an extraluminal mass of gastric fundus (white arrows). The lesion shows heterogeneous contrast enhancement, irregular margins and size > 10 cm. Axial (b) contrast-enhanced MDCT image in the arterial phase shows some over-centimetric serosal-based nodules located in mesenteric adipose tissue (white arrows)

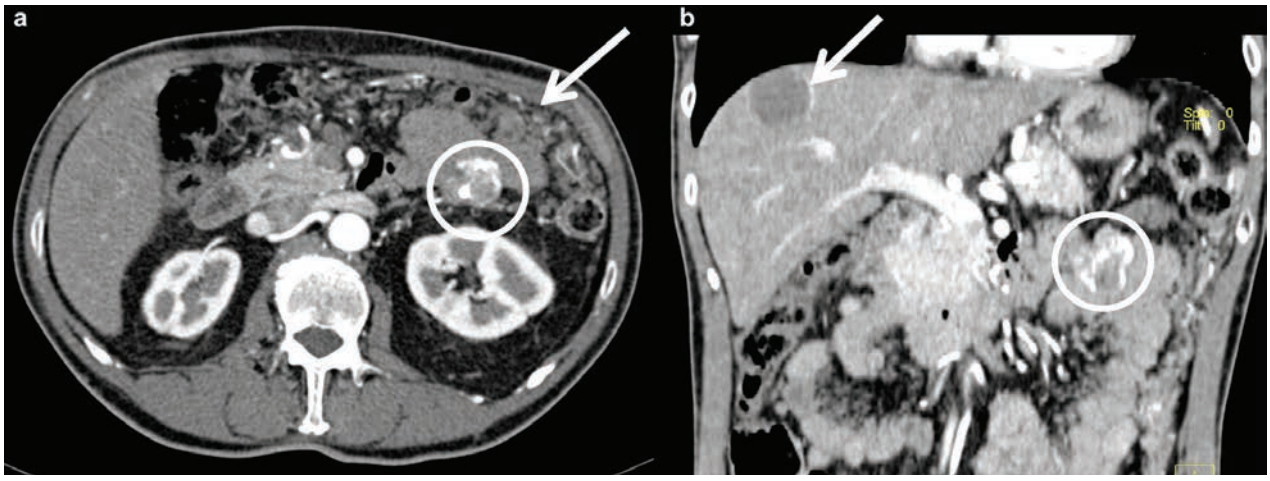

Figure 6. Axial (a) and coronal (b) contrast enhanced MDCT images in the arterial phase demonstrate a nodular mass of the jejunum (white circles). This GIST presents heterogeneous contrast enhancement, irregular margins and size < 5 cm. Just above, there is a diffuse reticular thickening of mesenteric adipose tissue (a, white arrow), suggestive for multiple serosal-based nodules. Furthermore coronal (b) contrast-enhanced MDCT image shows a hypovascular liver metastasis (white arrow)

belonging to the none and very low risk classes appear in most cases as lesions with a homogenous pattern of contrast enhancement (94, 96-104) (Table 1).

Even Levy et al. in their study notice that the degree of contrast enhancement, if high, was considered as a remarkable characteristic of tumor biological activity (74) (Table 2).

Table 1. Relationship between different diagnostic imaging features on MDCT and prognostic outcomes in GISTs

CT characteristics	Favorable prognosis	Intermediate prognosis	Unfavorable prognosis	Author, Year
Site	Stomach	Duodenum or rectum	Jejunum or ileum	Al-Thani et al., 2014
Size	<5 cm	>5 cm <10 cm	>10 cm	Miettenen et al., 2006
Single or multiple	Not related	Not related	Not related	Maldonado et al., 2018
Margins	Regular	/	Irregular	Iannicelli et al., 2009
Enhancement	Homogenous	/	Heterogeneous	Levy et al., 2003

Table 2. GISTs MDCT features that modify the homogeneity: hemorrhage, necrosis, calcifications, intralesional cavitation and cystic degeneration

Tumor characteristics	Characteristics	Prognosis	Author, Year
Hemorrhage	Area of hyper/iso/hypodensity	Unfavorable	Zhou et al., 2016
Necrosis	Area of hypodensity	Unfavorable	Lee et al., 2004
Calcifications	Focal or smudged hyperdensity	Not related	Maldonado et al., 2018
Intra-lesional cavitation	Intralesional hypodensity (air density)	Unfavorable	Kim et al., 2004
Cystic degeneration	Central area of hypodensity	Unfavorable	Maldonado et al., 2018

Discussion

To the best of our knowledge, only few studies had investigated the correlation of GISTs MDCT findings with pathology (74, 90-93). The study of Iannicelli et al. could be considered the first article where many features related to GISTs prognosis and behavior are compared with CT findings to assess whether any MDCT findings could be predictive or specific of the Miettinen classes of risk (80).

In this review we want to underline how unfavorable prognostic aspects are represented by the jejunal-ileal localization, tumor size greater than 10 cm, irregular margins, heterogeneous enhancement and other imaging features that modify homogeneity of lesion at non contrast-enhanced MDCT (hemorrhage, necrosis, intralesional cavitation and cystic degeneration) (87-91). Intermediate prognostic features are duodenal or rectal localization and lesion dimensions between 5 and 10 cm (31, 85). Favorable prognostic elements consist of gastric localization, tumor size below 5 cm, smooth margins, lesion with homogeneous density and homogeneous enhancement (74, 75, 91). The presence of single or multiple lesions and the intralesional calcifications (focal or smudged) do not seem to be correlated with the prognosis (91).

In conclusion MDCT imaging features are crucial in GISTs detection and contribute to the risk stratification evaluating localization and size of the tumor; moreover, MDCT morphological features could be correlated with pathological parameters like the mitotic rate which is the expression of the tumor biology. Therefore, MDCT parameters could give a first step orientation, before the pathological examination, of the biological behavior and the prognostic outcome of GISTs.

Ethical approval: This article does not contain any studies with human participants performed by any of the authors.

Conflict of interest: None to declare

References

1. Scola D, Bahoura L, Copelan A, Shirkhoda A, Sokhandon F. Getting the GIST: a pictorial review of the various patterns of presentation of gastrointestinal stromal tumors on imaging. Abdom Radiol (NY) 2017; 42: 1350-64.
2. Koumarianou A, Economopoulou P, Katsaounis P, et al. Gastrointestinal Stromal Tumors (GIST): A Prospective Analysis and an Update on Biomarkers and Current Treatment Concepts. Biomark Cancer 2015; 7: 1-7.
3. Sanders KM, Koh SD, Ward SM. Interstitial cells of cajal as pacemakers in the gastrointestinal tract. Annu Rev Physiol 2006; 68: 307-43.
4. Rubin BP, Heinrich MC, Corless CL. Gastrointestinal stromal tumour. Lancet 2007; 369: 1731-41.

5. DeMatteo RP, Lewis JJ, Leung D, Mudan SS, Woodruff JM, Brennan MF. Two hundred gastrointestinal stromal tumors: recurrence patterns and prognostic factors for survival. Ann Surg 2000; 231: 51-8.
6. Miettinen M, Sobin LH, Lasota J. Gastrointestinal stromal tumors of the stomach: a clinicopathologic, immunohistochemical, and molecular genetic study of 1765 cases with long-term follow-up. Am J Surg Pathol 2005; 29: 52-68.
7. Tworek JA, Appelman HD, Singleton TP, Greenson JK. Stromal tumors of the jejunum and ileum. Mod Pathol 1997; 10: 200-9.
8. Miettinen M, Sarlomo-Rikala M, Sobin LH, Lasota J. Gastrointestinal stromal tumors and leiomyosarcomas in the colon: a clinicopathologic, immunohistochemical, and molecular genetic study of 44 cases. Am J Surg Pathol 2000; 24: 1339-52.
9. Tworek JA, Goldblum JR, Weiss SW, Greenson JK, Appelman HD. Stromal tumors of the anorectum: a clinicopathologic study of 22 cases. Am J Surg Pathol 1999; 23: 946-54.
10. Tworek JA, Goldblum JR, Weiss SW, Greenson JK, Appelman HD. Stromal tumors of the abdominal colon: a clinicopathologic study of 20 cases. Am J Surg Pathol 1999; 23: 937-45.
11. Miettinen M, Sarlomo-Rikala M, Sobin LH, Lasota J. Esophageal stromal tumors: a clinicopathologic, immunohistochemical, and molecular genetic study of 17 cases and comparison with esophageal leiomyomas and leiomyosarcomas. Am J Surg Pathol 2000; 24: 211-22.
12. Reith JD, Goldblum JR, Lyles RH, Weiss SW. Extragastrointestinal (soft tissue) stromal tumors: an analysis of 48 cases with emphasis on histologic predictors of outcome. Mod Pathol 2000; 13: 577-85.
13. Miettinen M, Monihan JM, Sarlomo-Rikala M, et al. Gastrointestinal stromal tumors/smooth muscle tumors (GISTs) primary in the omentum and mesentery: clinicopathologic and immunohistochemical study of 26 cases. Am J Surg Pathol 1999; 23: 1109-18.
14. Romano L, Pinto A, Imaging of Alimentary Tract Perforation, Springer International Publishing, Springer International Publishing Switzerland, 2015.
15. Demetri GD, Benjamin R, Blanke CD, et al. NCCN Task Force report: optimal management of patients with gastrointestinal stromal tumor (GIST)--expansion and update of NCCN clinical practice guidelines. J Natl Compr Canc Netw 2004; 2 Suppl 1: S-1-26.
16. Agaimy A, Wunsch PH. Lymph node metastasis in gastrointestinal stromal tumours (GIST) occurs preferentially in young patients < or = 40 years: an overview based on our case material and the literature. Langenbecks Arch Surg 2009; 394: 375-81.
17. Miettinen M, Furlong M, Sarlomo-Rikala M, Burke A, Sobin LH, Lasota J. Gastrointestinal stromal tumors, intramural leiomyomas, and leiomyosarcomas in the rectum and anus: a clinicopathologic, immunohistochemical, and molecular genetic study of 144 cases. Am J Surg Pathol 2001; 25: 1121-33.
18. Gold JS, Gonen M, Gutierrez A, et al. Development and validation of a prognostic nomogram for recurrence-free survival after complete surgical resection of localised primary gastrointestinal stromal tumour: a retrospective analysis. Lancet Oncol 2009; 10: 1045-52.
19. Zhao X, Yue C. Gastrointestinal stromal tumor. J Gastrointest Oncol 2012; 3: 189-208.
20. Foo WC, Liegl-Atzwanger B, Lazar AJ. Pathology of gastrointestinal stromal tumors. Clin Med Insights Pathol 2012; 5: 23-33.
21. Miettinen M, Lasota J. Gastrointestinal stromal tumors--definition, clinical, histological, immunohistochemical, and molecular genetic features and differential diagnosis. Virchows Arch 2001; 438: 1-12.
22. Kindblom LG, Remotti HE, Aldenborg F, Meis-Kindblom JM. Gastrointestinal pacemaker cell tumor (GIPACT): gastrointestinal stromal tumors show phenotypic characteristics of the interstitial cells of Cajal. Am J Pathol 1998; 152: 1259-69.
23. Fletcher CD, Berman JJ, Corless C, et al. Diagnosis of gastrointestinal stromal tumors: A consensus approach. Hum Pathol 2002; 33: 459-65.
24. Sarlomo-Rikala M, Kovatich AJ, Barusevicius A, Miettinen M. CD117: a sensitive marker for gastrointestinal stromal tumors that is more specific than CD34. Mod Pathol 1998; 11: 728-34.
25. Palma BD, Guasco D, Pedrazzoni M, et al. Osteolytic lesions, cytogenetic features and bone marrow levels of cytokines and chemokines in multiple myeloma patients: Role of chemokine (C-C motif) ligand 20. Leukemia 2016; 30: 409-16.
26. Mol CD, Dougan DR, Schneider TR, et al. Structural basis for the autoinhibition and STI-571 inhibition of c-Kit tyrosine kinase. J Biol Chem 2004; 279: 31655-63.
27. Canu L, Pradella S, Rapizzi E, et al. Sunitinib in the therapy of malignant paragangliomas: report on the efficacy in a SDHB mutation carrier and review of the literature. Arch Endocrinol Metab 2017; 61: 90-97.
28. Kitayama H, Kanakura Y, Furitsu T, et al. Constitutively activating mutations of c-kit receptor tyrosine kinase confer factor-independent growth and tumorigenicity of factor-dependent hematopoietic cell lines. Blood 1995; 85: 790-8.
29. Nilsson B, Bumming P, Meis-Kindblom JM, et al. Gastrointestinal stromal tumors: the incidence, prevalence, clinical course, and prognostication in the preimatinib mesylate era--a population-based study in western Sweden. Cancer 2005; 103: 821-9.
30. Kang HC, Menias CO, Gaballah AH, et al. Beyond the GIST: mesenchymal tumors of the stomach. Radiographics 2013; 33: 1673-90.
31. Miettinen M, Lasota J. Gastrointestinal stromal tumors: pathology and prognosis at different sites. Semin Diagn Pathol 2006; 23: 70-83.
32. Masciocchi C, Arrigoni F, Ferrari F, et al. Uterine fibroid therapy using interventional radiology mini-invasive treatments: current perspective. Med Oncol 2017; 34: 52.

33. Ferrari F, Arrigoni F, Miccoli A, et al. Effectiveness of Magnetic Resonance-guided Focused Ultrasound Surgery (MRgFUS) in the uterine adenomyosis treatment: technical approach and MRI evaluation. Radiol Med 2016; 121: 153-61.
34. Gatta G, Parlato V, Di Grezia G, et al. Ultrasound-guided aspiration and ethanol sclerotherapy for treating endometrial cysts. Radiol Med 2010; 115: 1330-39.
35. Scialpi M, Cappabianca S, Rotondo A, et al. Pulmonary congenital cystic disease in adults. Spiral computed tomography findings with pathologic correlation and management. Radiol Med 2010; 115: 539-50.
36. Battipaglia G, Avilia S, Morelli E, Caranci F, Perna F, Camera A. Posterior reversible encephalopathy syndrome (PRES) during induction chemotherapy for acute myeloblastic leukemia (AML). Ann Hematol 2012; 91: 1327-28.
37. Briganti F, Leone G, Marseglia M, Cicala D, Caranci F, Maiuri F. P64 Flow Modulation Device in the treatment of intracranial aneurysms: Initial experience and technical aspects. J Neurointerv Surg 2016; 8: 173-80.
38. Arrigoni F, Barile A, Zugaro L, et al. Intra-articular benign bone lesions treated with Magnetic Resonance-guided Focused Ultrasound (MRgFUS): imaging follow-up and clinical results. Med Oncol 2017; 34: 55.
39. Cirillo M, Caranci F, Tortora F, et al. Structural neuroimaging in dementia. J Alzheimers Dis 2012; 29: 16-19.
40. Lagana D, Carrafiello G, Mangini M, et al. Radiofrequency ablation of primary and metastatic lung tumors: preliminary experience with a single center device. Surg Endosc 2006; 20: 1262-7.
41. Bertolini L, Vaglio A, Bignardi L, et al. Subclinical interstitial lung abnormalities in stable renal allograft recipients in the era of modern immunosuppression. Transplant Proc 2011; 43: 2617-23.
42. Sverzellati N, Calabrò E, Chetta A, et al. Visual score and quantitative CT indices in pulmonary fibrosis: Relationship with physiologic impairment. Radiol Med 2007; 112: 1160-72.
43. Carrafiello G, Dionigi G, Ierardi AM, et al. Efficacy, safety and effectiveness of image-guided percutaneous microwave ablation in cystic renal lesions Bosniak III or IV after 24 months follow up. Int J Surg 2013; 11 Suppl 1: S30-5.
44. Macchi M, Belfiore MP, Floridi C, et al. Radiofrequency versus microwave ablation for treatment of the lung tumours: LUMIRA (lung microwave radiofrequency) randomized trial. Med Oncol 2017; 34: 96.
45. Tarantini G, Favaretto E, Napodano M, et al. Design and methodologies of the postconditioning during coronary angioplasty in acute myocardial infarction (POST-AMI) trial. Cardiology 2010; 116: 110-16.
46. Regine G, Stasolla A, Miele V. Multidetector computed tomography of the renal arteries in vascular emergencies. Eur J Radiol 2007; 64: 83-91.
47. De Cecco CN, Buffa V, Fedeli S, et al. Preliminary experience with abdominal dual-energy CT (DECT): True versus virtual nonenhanced images of the liver. Radiol Med 2010; 115: 1258-66.
48. Buffa V, Solazzo A, D'Auria V, et al. Dual-source dual-energy CT: dose reduction after endovascular abdominal aortic aneurysm repair. Radiol Med 2014; 119: 934-41.
49. Cappabianca S, Iaselli F, Reginelli A, et al. Value of diffusion-weighted magnetic resonance imaging in the characterization of complex adnexal masses. Tumori 2013; 99: 210-17.
50. Brunese L, Romeo A, Iorio S, et al. Thyroid B-flow twinkling sign: a new feature of papillary cancer. Eur J Endocrinol 2008; 159: 447-51.
51. Mocchegiani F, Vincenzi P, Coletta M, et al. Prevalence and clinical outcome of hepatic haemangioma with specific reference to the risk of rupture: A large retrospective cross-sectional study. Dig Liver Dis 2016; 48: 309-14.
52. di Giacomo V, Trinci M, van der Byl G, Catania VD, Calisti A, Miele V. Ultrasound in newborns and children suffering from non-traumatic acute abdominal pain: imaging with clinical and surgical correlation. J Ultrasound 2015; 18: 385-93.
53. Iacobellis F, Segreto T, Berritto D, et al. A rat model of acute kidney injury through systemic hypoperfusion evaluated by micro-US, color and PW-Doppler. Radiol Med 2018;
54. Dionigi G, Dionigi R, Rovera F, et al. Treatment of high output entero-cutaneous fistulae associated with large abdominal wall defects: single center experience. Int J Surg 2008; 6: 51-6.
55. Ierardi AM, Lucchina N, Petrillo M, et al. Systematic review of minimally invasive ablation treatment for locally advanced pancreatic cancer. Radiol Med 2014; 119: 483-98.
56. Lo Re G, Cappello M, Tudisca C, et al. CT enterography as a powerful tool for the evaluation of inflammatory activity in Crohn's disease: Relationship of CT findings with CDAI and acute-phase reactants. Radiol Med 2014; 119: 658-66.
57. Salvolini L, Urbinati C, Valeri G, Ferrara C, Giovagnoni A. Contrast-enhanced MR cholangiography (MRCP) with GD-EOB-DTPA in evaluating biliary complications after surgery. Radiol Med 2012; 117: 354-68.
58. Cappabianca S, Reginelli A, Monaco L, Del Vecchio L, Di Martino N, Grassi R. Combined videofluoroscopy and manometry in the diagnosis of oropharyngeal dysphagia: Examination technique and preliminary experience. Radiol Med 2008; 113: 923-40.
59. Maggialetti N, Capasso R, Pinto D, et al. Diagnostic value of computed tomography colonography (CTC) after incomplete optical colonoscopy. Int J Surg 2016; 33 Suppl 1: S36-44.
60. Mandato Y, Reginelli A, Galasso R, Iacobellis F, Berritto D, Cappabianca S. Errors in the Radiological Evaluation of the Alimentary Tract: Part I. Semin Ultrasound CT MR 2012; 33: 300-07.
61. Reginelli A, Mandato Y, Solazzo A, Berritto D, Iacobellis F, Grassi R. Errors in the Radiological Evaluation of the Alimentary Tract: Part II. Semin Ultrasound CT MR 2012; 33: 308-17.
62. Schicchi N, Valeri G, Moroncini G, et al. Myocardial perfusion defects in scleroderma detected by contrast-enhanced

cardiovascular magnetic resonance. Radiol Med 2014; 119: 885-94.
63. Maggialetti N, Ferrari C, Minoia C, et al. Role of WB-MR/DWIBS compared to 18F-FDG PET/CT in the therapy response assessment of lymphoma. Radiol Med 2016; 121: 132-43.
64. Cortellini A, Verna L, Porzio G, et al. Predictive value of skeletal muscle mass for immunotherapy with nivolumab in non-small cell lung cancer patients: A "hypothesis-generator" preliminary report. Thorac Cancer 2019; 10: 347-51.
65. Cortellini A, Palumbo P, Porzio G, et al. Single-institution study of correlations between skeletal muscle mass, its density, and clinical outcomes in non-small cell lung cancer patients treated with first-line chemotherapy. Thorac Cancer 2018; 9: 1623-30.
66. Splendiani A, Perri M, Marsecano C, et al. Effects of serial macrocyclic-based contrast materials gadoterate meglumine and gadobutrol administrations on gadolinium-related dentate nuclei signal increases in unenhanced T1-weighted brain: a retrospective study in 158 multiple sclerosis (MS) patients. Radiol Med 2018; 123: 125-34.
67. Grassi R, Rambaldi PF, Di Grezia G, et al. Inflammatory bowel disease: Value in diagnosis and management of MDCT-enteroclysis and 99mTc-HMPAO labeled leukocyte scintigraphy. Abdom Imaging 2011; 36: 372-81.
68. Tedeschi E, Caranci F, Giordano F, Angelini V, Cocozza S, Brunetti A. Gadolinium retention in the body: what we know and what we can do. Radiol Med 2017; 122: 589-600.
69. Cappabianca S, Porto A, Petrillo M, et al. Preliminary study on the correlation between grading and histology of solitary pulmonary nodules and contrast enhancement and [18F] fluorodeoxyglucose standardised uptake value after evaluation by dynamic multiphase CT and PET/CT. J Clin Pathol 2011; 64: 114-19.
70. Valentini V, Buquicchio GL, Galluzzo M, et al. Intussusception in Adults: The Role of MDCT in the Identification of the Site and Cause of Obstruction. Gastroenterol Res Pract 2016; 2016: 5623718-18.
71. Pradella S, Lucarini S, Colagrande S. Liver lesion characterization: the wrong choice of contrast agent can mislead the diagnosis of hemangioma. AJR Am J Roentgenol 2012; 199: W662.
72. Sforza V, Martinelli E, Ciardiello F, et al. Mechanisms of resistance to anti-epidermal growth factor receptor inhibitors in metastatic colorectal cancer. World J Gastroenterol 2016; 22: 6345-61.
73. Valeri G, Mazza FA, Maggi S, et al. Open source software in a practical approach for post processing of radiologic images. Radiol Med 2015; 120: 309-23.
74. Levy AD, Remotti HE, Thompson WM, Sobin LH, Miettinen M. Gastrointestinal stromal tumors: radiologic features with pathologic correlation. Radiographics 2003; 23: 283-304, 456; quiz 532.
75. Iannicelli E, Scavone G, Speranza A, Sessa B, David V. [MDCT in GIST evaluation.]. Clin Ter 2009; 160: 201-6.
76. Sharp RM, Ansel HJ, Keel SB. Best cases from the AFIP: gastrointestinal stromal tumor. Armed Forces Institute of Pathology. Radiographics 2001; 21: 1557-60.
77. Scatarige JC, Fishman EK, Jones B, Cameron JL, Sanders RC, Siegelman SS. Gastric leiomyosarcoma: CT observations. J Comput Assist Tomogr 1985; 9: 320-7.
78. Sandrasegaran K, Rajesh A, Rushing DA, Rydberg J, Akisik FM, Henley JD. Gastrointestinal stromal tumors: CT and MRI findings. Eur Radiol 2005; 15: 1407-14.
79. Ghanem N, Altehoefer C, Furtwangler A, et al. Computed tomography in gastrointestinal stromal tumors. Eur Radiol 2003; 13: 1669-78.
80. Iannicelli E, Carbonetti F, Federici GF, et al. Evaluation of the Relationships Between Computed Tomography Features, Pathological Findings, and Prognostic Risk Assessment in Gastrointestinal Stromal Tumors. J Comput Assist Tomogr 2017; 41: 271-78.
81. Hong X, Choi H, Loyer EM, Benjamin RS, Trent JC, Charnsangavej C. Gastrointestinal stromal tumor: role of CT in diagnosis and in response evaluation and surveillance after treatment with imatinib. Radiographics 2006; 26: 481-95.
82. Burkill GJ, Badran M, Al-Muderis O, et al. Malignant gastrointestinal stromal tumor: distribution, imaging features, and pattern of metastatic spread. Radiology 2003; 226: 527-32.
83. Faggian A, Fracella MR, D'Alesio G, et al. Small-Bowel Neoplasms: Role of MRI Enteroclysis. Gastroenterol Res Pract 2016; 2016: 9686815.
84. Khoo CY, Chai X, Quek R, Teo MCC, Goh BKP. Systematic review of current prognostication systems for primary gastrointestinal stromal tumors. Eur J Surg Oncol 2018; 44: 388-94.
85. Al-Thani H, El-Menyar A, Rasul KI, et al. Clinical presentation, management and outcomes of gastrointestinal stromal tumors. Int J Surg 2014; 12: 1127-33.
86. Min KW, Leabu M. Interstitial cells of Cajal (ICC) and gastrointestinal stromal tumor (GIST): facts, speculations, and myths. J Cell Mol Med 2006; 10: 995-1013.
87. Zhou C, Duan X, Zhang X, Hu H, Wang D, Shen J. Predictive features of CT for risk stratifications in patients with primary gastrointestinal stromal tumour. Eur Radiol 2016; 26: 3086-93.
88. Lee CM, Chen HC, Leung TK, Chen YY. Gastrointestinal stromal tumor: Computed tomographic features. World J Gastroenterol 2004; 10: 2417-8.
89. Tang L, Li J, Li ZY, et al. MRI in predicting the response of gastrointestinal stromal tumor to targeted therapy: a patient-based multi-parameter study. BMC Cancer 2018; 18: 811.
90. Kim HC, Lee JM, Choi SH, et al. Imaging of gastrointestinal stromal tumors. J Comput Assist Tomogr 2004; 28: 596-604.
91. Maldonado FJ, Sheedy SP, Iyer VR, et al. Reproducible imaging features of biologically aggressive gastrointestinal stromal tumors of the small bowel. Abdom Radiol (NY) 2018; 43: 1567-74.

92. Pinaikul S, Woodtichartpreecha P, Kanngurn S, Leelakiatpaiboon S. 1189 Gastrointestinal stromal tumor (GIST): computed tomographic features and correlation of CT findings with histologic grade. J Med Assoc Thai 2014; 97: 1189-98.
93. Baheti AD, Shinagare AB, O'Neill AC, et al. MDCT and clinicopathological features of small bowel gastrointestinal stromal tumours in 102 patients: a single institute experience. Br J Radiol 2015; 88: 20150085.
94. Tateishi U, Hasegawa T, Satake M, Moriyama N. Gastrointestinal stromal tumor. Correlation of computed tomography findings with tumor grade and mortality. J Comput Assist Tomogr 2003; 27: 792-8.
95. Rossi S, Miceli R, Messerini L, et al. Natural history of imatinib-naive GISTs: a retrospective analysis of 929 cases with long-term follow-up and development of a survival nomogram based on mitotic index and size as continuous variables. Am J Surg Pathol 2011; 35: 1646-56.
96. Horton KM, Juluru K, Montogomery E, Fishman EK. Computed tomography imaging of gastrointestinal stromal tumors with pathology correlation. J Comput Assist Tomogr 2004; 28: 811-7.
97. Da Ronch T, Modesto A, Bazzocchi M. Gastrointestinal stromal tumour: spiral computed tomography features and pathologic correlation. Radiol Med 2006; 111: 661-73.
98. Kim HC, Lee JM, Kim KW, et al. Gastrointestinal stromal tumors of the stomach: CT findings and prediction of malignancy. AJR Am J Roentgenol 2004; 183: 893-8.
99. Bozzetti C, Nizzoli R, Tiseo M, et al. ALK and ROS1 rearrangements tested by fluorescence in situ hybridization in cytological smears from advanced non-small cell lung cancer patients. Diagnostic Cytopathology, vol. 43, p. 941-946, ISSN: 8755-1039, doi: 10.1002/dc.23318
100. De Filippo M, Onniboni M, Rusca M, et al. (2008). Advantages of multidetector row CT with multiplanar reformation in guiding percutaneous lung biopsies. RAD. MED, vol. 113, p. 945-953, ISSN: 0033-8362, doi: 10.1007/s11547-008-0325-y
101. Gafà G, Sverzellati N, Bonati E, et al (2012). Follow-up in pulmonary sarcoidosis: comparison between HRCT and pulmonary function tests. RAD. MED, vol. 117, p. 968-978, ISSN: 0033-8362, doi: 10.1007/s11547-012-0827-5
102. Barile A, Bruno F, Mariani S, et al. What can be seen after rotator cuff repair: a brief review of diagnostic imaging findings. Musculoskelet Surg. 2017 Mar;101(Suppl 1):3-14. doi: 10.1007/s12306-017-0455-2. Epub 2017 Feb 13. Review.
103. De Filippo M, Gira F, Corradi D, Sverzellati N, Zompatori M, Rossi C. (2011). Benefits of 3D technique in guiding percutaneous retroperitoneal biopsies. RAD. MED, vol. 116(3), p. 407-416, ISSN: 0033-8362, doi: 10.1007/s11547-010-0604-2
104. Ulusan S, Koc Z, Kayaselcuk F. Gastrointestinal stromal tumours: CT findings. Br J Radiol 2008; 81: 618-23.

Received: 26 March 2019
Accepted: 4 April 2019
Correspondence:
Silvia Pradella, MD
Department of Radiology - Careggi University Hospital
L.go G.A. Brambilla, 3 - 50134 Florence, Italy
E-mail: pradella3@yahoo.it